Electronic Supplementary Information

Calamitic and discotic liquid crystalline phases for mesogens with triangular core

Jadwiga Szydłowska, Adam Krówczyński, Ewa Górecka, Damian Pociecha*

Experimental

Synthesis of materials

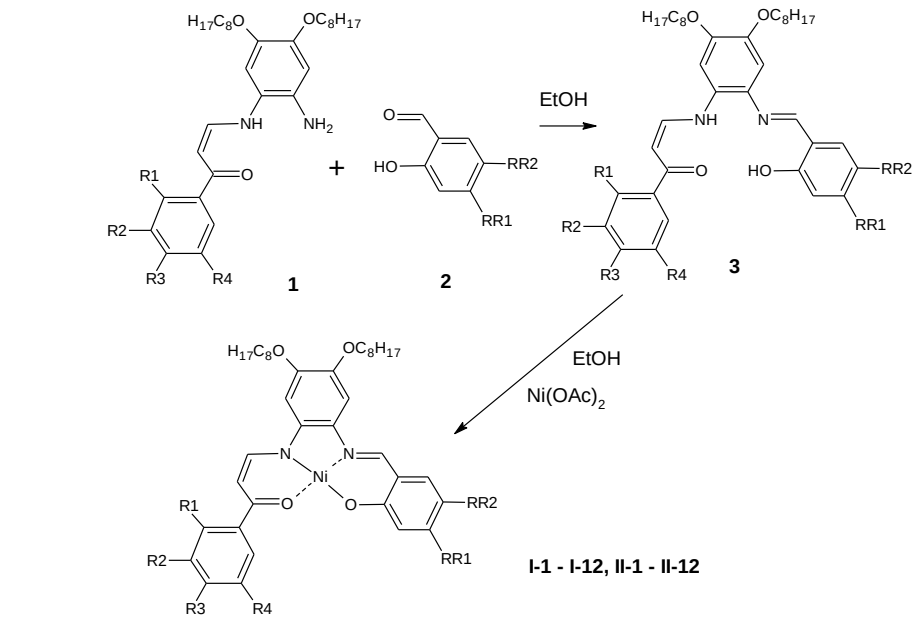

a)

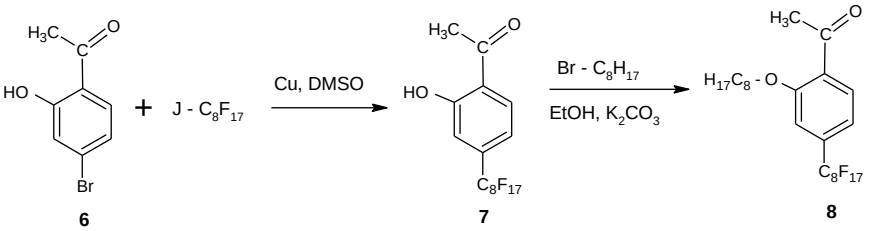

b)

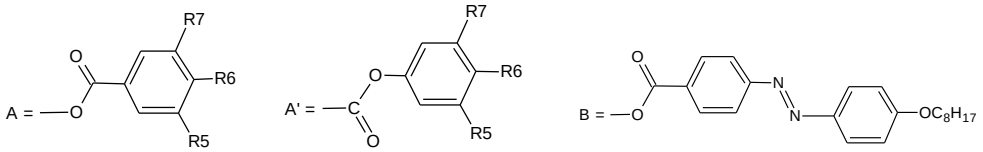

c)

Scheme SI 1. Synthesis of compounds a) **I-1 – I-12** and **II-1 – II-12**, b) synthesis of compound **2-octyloxy-4-(perfluoro-n-octyl)acetophenone**, (**8**); c) structure of substituents RR1 and RR2

Electronic Supplementary Information

Chemical procedures

The chemical procedure to synthesize the compounds **I-1 – I-12** and **II-1 – II-12** are shown in Scheme SI 1a). The preparation of group of substrates (**1**) was presented in Ref. 1 except where R1 and R3 are R1 = OC_8H_{17} and R3 = C_8F_{17}. **2-octyloxy-4-(perfluoro-n-octyl)acetophenone** (**8**) compound necessary for the synthesis of the materials with perfluorinated chain was prepared analogously to in Ref. 2. (Scheme SI 1b): A suspension of 2-hydroxy-4-bromoacetophenone (**6**) (21.5 g, 100 mmol), perfluoro-n-octyl iodide (62 g, 110 mmol) and powdered copper (32 g, 500 mmol) in DMSO (100 ml) was heated overnight with stirring under argon atmosphere at 110 ºC. From the hot mixture the excess of the copper powder was filtered out and the filtrate was diluted with water (400 ml) and the precipitated **2-hydroxy -4-(perfluoro-n -octyl)acetophenone** (**7**) was separated (550 g, ca. 100 mmol). In this compound (**7**) hydroxy group was replaced by octyloxy group in a reaction with mixture of n-octyl bromide (22 g, 110 mmol), potassium carbonate (15.5 g, 110 mmol) and ethanol (400 ml). The reaction suspension was distilled with water vapor to remove ethanol and excess of octyl bromide. After cooling the precipitate (**8**) was filtered, dried and re-crystallized from hexane.

2-hydroxy -4-(perfluoro-n-octyl)acetophenone (**7**) *^{1}H NMR* (400 MHz, $CDCl_3$): δ = 2.69 (s, 3H); 7.12 (dd, J=1.7 Hz, J=8.4 Hz, H); 7.24 (d, J=1.7 Hz, H); 7.87 (d, J=8.4 Hz, H); 12.27 (s, H). *^{19}F NMR* (400 MHz, $CDCl_3$): δ = -126.15 (m, 2F); -122.75 (m, 2F); -121.88 (m, 6F); -121.25 (m, 2F); -111.71 (t, J=14.5 Hz, 2F); -80.81 (t, J=9.9 Hz, 3F).

2-octyloxy-4-(perfluoro-n-octyl)acetophenone (**8**) *^{1}H NMR* (400 MHz, $CDCl_3$): δ = 0.86-1.92 (m, 15H); 2.65 (s, 3H); 4.10 (t, J=6.5 Hz, 2H); 7.12 (broad s, H); 7.19 (broad d, J=8.1Hz, H); 7.80 (d, J=8.1 Hz, H). *^{19}F NMR* (400 MHz, $CDCl_3$): δ =-126.14 (m, 2F); -122.74 (m, 2F); -121.89 (m, 6F); -121.24 (m, 2F); -111.08 (t, J=14.3 Hz, 2F); -80.81 (t, J=9.7 Hz, 3F).

1-{3'-[2''-octyloxy-4''- (perfluoro-n-octyl)phenyl]-3'-oxo-1'-propenylamino}-2-amino-4, 5-dioctyloxybenzene (**1**, for R1 = -OC_8H_{17}, R3=C_8F_{17} R2=R4=H) *^{1}H NMR* (400 MHz, $CDCl_3$): δ =0.86-1.88 (m, 45H); 3.53 (broad s, 2H); 3.93 (t, J=6.6 Hz, 4H); 4.08 (t, J=6.5 Hz, 2H); 6.10 (d, J=7.5 Hz, H); 6.41 (s, 1H); 6.71 (s, 1H); 6.10 (broad s, H); 7.23 (broad d, J=8.0Hz, H); 7.30 (dd, J=7.5 Hz, J=12.2 Hz, H); 7.86 (d, J=8.0 Hz, H); 12.04 (d, J=12.2 Hz, H). *^{19}F NMR* (400 MHz, $CDCl_3$): δ =-126.14 (m, 2F); -122.73 (m, 2F);-121.85 (m, 6F); -121.24 (m, 2F); -110.79 (t, J=14.1 Hz, 2F); -80.80 (t, J=9.8 Hz, 3F).

The group of substrates (**2**) of the reaction a) (Scheme SI 1) can have attached tree types of substituents: A, A' and B (Scheme Si 1c)). The related aromatic acids AH, A'H and BH are available as commercial products. The preparation of the 4- or 5-substituted salicylic aldehyde (**2**) where RR1 = A and RR2 = H was described in Ref 3 as well as for RR1 = H and RR2 = A or A' – in Ref 4. Some of the compounds of group **2** used in the reaction a) have not be synthesized yet, so their NMR spectra are given:

4-formyl-3-hydroxyphenyl-3,4,5-tris(octyloxy)benzoate (**2**, for R11=A, RR2=H, R5=R6=R7= –OC_8H_{17}) *^{1}H NMR* (400 MHz, $CDCl_3$): δ = 0.85-1.86 (m, 45H); 3.97-4.09 (m, 6H); 7.04 (d, J=8.0 Hz, H); 7.37 (dd, J=2.8 Hz, J=9.0 Hz, H); 7.39 (s, 2H); 7.42 (d, J=2.8 Hz, H); 9.87 (s, H); 10.94 (s, H).

4-formyl-3-hydroxyphenyl-4-(3,6-dioxaheptyloxy)benzoate (**2**, for R11=A, RR2=H, R6= –$O(CH_2)_2O(CH_2)_2OCH_3$, R5=R7=H) *^{1}H NMR* (400 MHz, $CDCl_3$): δ =3.40 (s, 3H); 3.57-3.62 (m, 2H); 3.72-3.76 (m, 2H); 3.88-3.92 (m, 2H); 4.21-4.25 (m, 2H); 6.88 (d, J=1.7 Hz, H); 6.91 (dd, J=1.7 Hz, J=8.4 Hz, H); 7.00 and 8.12 (AA'BB', J=8.7 Hz, 4H); 7.61 (d, J=8.4 Hz, H); 9.88 (s, H); 11.25 (s, H).

4-formyl-3-hydroxyphenyl-4-(4'-octyloxyphenylazo)benzoate (**2**, for R11=B, RR2=H) *^{1}H NMR* (400 MHz, $CDCl_3$): δ =0.84-1.86 (m, 15H); 4.05 (t, J=6.6 Hz, 2H); 6.92 (d, J=2.1 Hz, H); 6.95 (dd, J=2.1 Hz, J=8.4 Hz, H); 7.02 and 7.96 (AA'BB', J=9.1 Hz, 4H); 7.62 (d, J=8.4 Hz, H); 7.97 and 8.29 (AA'BB', J=8.7 Hz, 4H); 9.89 (s, H); 11.25 (s, H).

3-formyl-4-hydroxyphenyl-4-octyloxbenzoate (**2**, for R11=H, RR2=A, R6= –OC_8H_{17}, R5=R7=H) *^{1}H NMR* (400 MHz, $CDCl_3$): δ = 0.85–1.87 (m, 15H); 4.04 (t, J=6.6 Hz, 2H); 6.98 and 8.12 (AA'BB', J=9.0 Hz, 4H); 7.04 (d, J=9.0 Hz, H); 7.37 (dd, J=2.9 Hz, J=9.0 Hz, H); 7.44 (d, J=2.9 Hz, H); 9.87 (s, H); 10.34 (s, H).

3-formyl-4-hydroxyphenyl-3,4,5-tris(octyloxy)benzoate (**2**, for R11=H, RR2=A, R5=R6=R7= –OC_8H_{17}) *^{1}H NMR* (400 MHz, $CDCl_3$): δ =0.85–1.86 (m, 45H); 3.97-4.09 (m, 6H); 7.04 (d, J=9.0 Hz, H); 7.37 (dd, J=2.8 Hz, J=9.0 Hz, H); 7.39 (s, 2H); 7.42 (d, J=2.8 Hz, H); 9.87 (s, H); 10.94 (s, H).

3-formyl-4-hydroxyphenyl-4-(3,6-dioxaheptyloxy)benzoate (**2**, for R11=H, RR2=A, R6= –$O(CH_2)_2O(CH_2)_2OCH_3$, R5=R7=H)) *^{1}H NMR* (400 MHz, $CDCl_3$): δ =3.38 (s, 3H); 3.56-3.60 (m, 2H); 3.71-3.74 (m, 2H); 3.87-3.91 (m, 2H); 4.20-4.24 (m, 2H); 6.97 and 8.12 (AA'BB', J=9.0 Hz, 4H); 7.02 (d, J=9.0 Hz, H); 7.35 (dd, J=2.8 Hz, J=9.0 Hz, H); 7.42 (d, J=2.8 Hz, H); 9.85 (s, H); 10.92 (s, H).

Electronic Supplementary Information

4-octyloxyphenyl-3-formyl-4-hydroxybenzoate (**2**, for R11=H, RR2=A', R6= $-OC_8H_{17}$, R5=R7=H) *^{1}H NMR* (400 MHz, $CDCl_3$): δ=0.85−1.87 (m, 15H); 3.96 (t, J=6.6 Hz, 2H); 6.93 and 7.11 (AA'BB', J=9.1 Hz, 4H); 7.10 (d, J=9.0 Hz, H); 8.33 (dd, J=2.2 Hz, J=9.0 Hz, H); 8.47 (d, J=2.2 Hz, H); 9.99 (s, H); 11.48 (s, H).

3-formyl-4-hydroxyphenyl- 4-(4'-octyloxyphenylazo)benzoate (**2**, for R11=H, RR2=B) *^{1}H NMR* (400 MHz, $CDCl_3$): δ=0.88−1.86 (m, 15H); 4.04 (t, J=6.6 Hz, 2H); 7.01 and 7.95 (AA'BB', J=9.0 Hz, 4H); 7.05 (d, J=8.9 Hz, H); 7.40 (dd, J=2.9 Hz, J=8.9 Hz, H); 7.47 (d, J=2.9 Hz, H); 7.97 and 8.30 (AA'BB', J=8.9 Hz, 4H); 9.87 (s, H); 10.95 (s, H).

Complexes I-1 – I-12 and **II-1 – II-12:** Equimolar amount (about 1 mmol) of substrates (**1**) and (**2**) were dissolved in hot ethanol with 3 - 4 droplets of acetic acid and the mixture was boiled for 10 min. To the resultant ligand (**3**) without separation nickel acetate dissolved in methanol was added and boiled for 5 min. After cooling sediment of a nickel complex (one from **I-1 – I-12** and **II-1 – II-12** compounds) was filtered, dried and purified in thin layer chromatography (silica gel and dichloromethane)

I-1: *Elemental analysis* for $C_{61}H_{84}N_2O_8Ni$ (1032.02 g/mol); calculated; C 70.99; H 8.20; N 2.71; found C 70.92; H 8.25; N 2.65;
^{1}H NMR (400 MHz, $CDCl_3$): δ=0.85−1.87 (m, 60H); 3.89 (t, J=6.6 Hz, 2H); 3.92-4.00 (m, 4H); 4.04 (t, J=6.6 Hz, 2H); 5.97 and 7.22 (AB, J=6.7 Hz, 2H); 6.51 (dd, J=2.2 Hz, J=8.7 Hz, H); 6.80 (s, H); 6.85 and 7.77 (AA'BB', J=9.0 Hz, 4H); 6.88 (d, J=2.2 Hz, H); 6.97 and 8.13 (AA'BB', J=9.0 Hz, 4H); 7.05 (s, H); 7.29 (d, J=8.7 Hz, H); 7.88 (s, H).

I-2: *Elemental analysis* for $C_{69}H_{100}N_2O_9Ni$ (1160.23 g/mol); calculated; C 71.43; H 8.69; N 2.41; found C 71.34; H 8.72; N 2.34;
^{1}H NMR (400 MHz, $CDCl_3$): δ=0.85−1.86 (m, 75H); 3.93-4.07 (m, 10H); 6.39 (d, J=2.3 Hz, H); 6.49-6.53 (m, 2H); 6.59 (dd, J=2.2 Hz, J=8.7 Hz, H); 6.93 (s, H); 6.96 and 8.12 (AA'BB', J=9.0 Hz, 4H); 6.99 (d, J=2.2 Hz, H); 7.12 (s, H); 7.30 (d, J=7.1 Hz, H); 7.38 (d, J=8.7 Hz, H); 7.91 (d, J=8.8 Hz, H); 8.00 (s, H).

I-3: *Elemental analysis* for $C_{69}H_{100}N_2O_9Ni$ (1160.23 g/mol); calculated; C 71.43; H 8.69; N 2.41; found C 71.45; H 8.40; N 2.52;
^{1}H NMR (400 MHz, $CDCl_3$): δ=0.82−1.86 (m, 75H); 3.91-4.06 (m, 10H); 4.62 and 7.33 (AB, J=6.7 Hz, 2H); 6.80 (d, J=9.0 Hz, H); 6.86 (dd, J=3.1 Hz, J=9.0 Hz, H); 6.91 (d, J=2.2 Hz, H); 6.93 (s, H); 6.95 and 8.11 (AA'BB', J=8.9 Hz, 4H); 7.12 (s, H); 7.37 (d, J=8.7 Hz, H); 7.99 (s, H).

I-4: *Elemental analysis* for $C_{77}H_{116}N_2O_{10}Ni$ (1288.44 g/mol); calculated; C 71.78; H 9.07; N 2.17; found C 71.66; H 9.01; N 2.25;
^{1}H NMR (400 MHz, $CDCl_3$): δ=0.83−1.84 (m, 90H); 3.91-4.06 (m, 12H); 4.38 and 7.24 (AB, J=6.6 Hz, 2H); 6.55 (dd, J=2.0 Hz, J=8.6 Hz, H); 6.64 and 7.50 (AB, J=9.0 Hz, 2H); 6.87 (s, H); 6.92 (broad s, H); 6.96 and 8.12 (AA'BB', J=9.0 Hz, 4H); 7.09 (s, H); 7.34 (d, J=8.6 Hz, H); 7.94 (s, H).

I-5: *Elemental analysis* for $C_{69}H_{83}F_{17}N_2O_8Ni$ (1450.07 g/mol); calculated; C 57.15; H 5.77; N 1.93; found C 57.03; H 5.84; N 1.89;
^{1}H NMR (400 MHz, $CDCl_3$): δ=0.83−1.86 (m, 60H); 3.94–4.06 (m, 16H); 6.36 and 7.33 (AB, J=6.6 Hz, 2H); 6.57 (dd, J=2.2 Hz, J=8.7 Hz, H); 6.90 (s, H); 6.92 (d, J=2.2 Hz, H); 6.96 and 8.11 (AA'BB', J=9.0 Hz, 4H); 7.02 (broad s, H); 7.09 (s, H); 7.17 (broad d, J=8.2 Hz, H); 7.34 (d, J=8.7 Hz, H); 7.92 (s, H); 7.95 (d, J=8.2 Hz, H). *^{19}F NMR* (400 MHz, $CDCl_3$): δ=-126.14 (m, 2F); -122.73 (m, 2F); -121.85 (m, 6F); -121.22 (m, 2F); -110.84 (t, J=14.3 Hz, 2F); -80.77 (t, J=9.9 Hz, 3F).

I-6: *Elemental analysis* for $C_{85}H_{132}N_2O_{11}Ni$ (1416.65 g/mol); calculated; C 72.07; H 9.39; N 1.98; found C 71.92; H 9.27; N 2.00;
^{1}H NMR (400 MHz, $CDCl_3$): δ=0.84–1.88 (m, 105H); 3.94–4.08 (m, 14H); 6.39 (d, J=2.2 Hz, H); 6.47-6.51 (m, 2H); 6.53 (dd, J=2.2 Hz, J=8.7 Hz, H); 6.89 (s, H); 6.93 (d, J=2.1 Hz, H); 7.11 (s, H); 7.25 (d, J=7.0 Hz, H); 7.36 (d, J=8.8 Hz, H); 7.39 (s, 2H); 7.88 (d, J=8.7Hz, H); 7.97 (s, H).

I-7: *Elemental analysis* for $C_{93}H_{148}N_2O_{12}Ni$ (1544.86 g/mol); calculated; C 72.30; H 9.66; N 1.81; found C 72.37; H 9.72; N 1.77;
^{1}H NMR (400 MHz, $CDCl_3$): δ=0.83−1.86 (m, 120H); 3.92-4.08 (m, 16H); 6.39 and 7.28 (AB, J=7.4 Hz, 2H); 6.53 (dd, J=2.1 Hz, J=8.7 Hz, H); 6.65 and 7.50 (AB, J=9.0 Hz, 2H); 6.89 (s, H); 6.91 (d, J=2.1 Hz, H); 7.11 (s, H); 7.35 (d, J=8.7 Hz, H); 7.39 (s, 2H); 7.96 (s, H).

I-8: *Elemental analysis* for $C_{85}H_{115}F_{17}N_2O_{10}Ni$ (1706.49 g/mol); calculated; C 59.81; H 6.79; N 1.64; found C 59.91; H 6.85; N 1.59;

^{1}H NMR (400 MHz, $CDCl_3$): δ=0.84–1.88 (m, 90H); 3.97-4.08 (m, 12H); 6.39 (d, J=6.5 Hz, H); 6.57 (dd, J=2.2 Hz, J=8.7 Hz, H); 6.93-6.95 (m, 2H); 7.03 (broad s, H); 7.11 (s, H); 7,18 (broad d, J=8.2 Hz, H); 7.35-7.40 (m, 4H); 7.94-7.98 (m, 2H). *^{19}F NMR* (400 MHz, $CDCl_3$): δ=-126.12 (m, 2F); -122.71 (m, 2F);-121.85 (m, 6F); -121.19 (m, 2F); -110.84 (t, J=14.3 Hz, 2F); -80.77 (t, J=9.9 Hz, 3F).

I-9: *Elemental analysis* for $C_{66}H_{77}F_{17}N_2O_{10}Ni$ (1439.99 g/mol); calculated; C 55.05; H 5.39; N 1.95; found C 54.98; H 5.42; N 2.01;
^{1}H NMR (400 MHz, $CDCl_3$): δ=0.83–1.86 (m, 45H); 3.40 (s, 3H); 3.57-3.62 (m, 2H); 3.71-3.76 (m, 2H); 3.88-4.05 (m, 6H); 4.21-4.25 (m, 2H); 6.34 and 7.28 (AB, J=6.6 Hz, 2H); 6.53 (dd, J=2.1 Hz, J=8.8 Hz, H); 6.85 (s, H); 6.87 (d, J=2.1 Hz, H); 6.97-7.01 (m, 3H); 6.06 (s, H); 7.15 (broad d, J=8.1 Hz, H); 7.31 (d, J=8.8 Hz, H); 7.86 (s, H); 7.94 (d, J=8.1 Hz, H); 8.12 (d, J=8.9 Hz, 2H). *^{19}F NMR* (400 MHz, $CDCl_3$): δ=-126.13 (m, 2F); -122.75 (m, 2F);-121.80 (m, 6F); -121.24 (m, 2F); -110.84 (t, J=14.3 Hz, 2F); -80.80 (t, J=9.9 Hz, 3F).

I-11: *Elemental analysis* for $C_{75}H_{104}N_4O_9Ni$ (1264.34 g/mol); calculated; C 71.25; H 8.29; N 4.43; found C 71.13; H 8.27; N 4.40;
^{1}H NMR (400 MHz, $CDCl_3$): δ=0.85–1.85 (m, 75H); 3.94-4.08 (m, 10H); 6.39 (d, J=2.2 Hz, H); 6.49-6.53 (m, 2H); 6.60 (dd, J=2.2 Hz, J=8.8 Hz, H); 6.89 (s, H); 6.97-7.04 (m, 3H); 7.11 (s, H); 7.27 (d, J=6.8 Hz, H); 7.39 (d, J=8.8 Hz, H);); 7.91 (d, J=8.8 Hz, H); 7.94-8.00 (m, 5H); 8.31 (d, J=8.6 Hz, 2H).

I-12: *Elemental analysis* for $C_{75}H_{87}F_{17}N_4O_8Ni$ (1554.18 g/mol); calculated; C 57.96; H 5.64; N 3.61; found C 58.02; H 5.70; N 3.57;
^{1}H NMR (400 MHz, $CDCl_3$): δ=0.83–1.84 (m, 60H); 3.92-4.08 (m, 8H); 6.37 and 7.30 (AB, J=6.7 Hz, H); 6.58 (dd, J=2.2 Hz, J=8.7 Hz, H); 6.87 (s, H); 6.93 (d, J=2.2 Hz, H); 6.99-7.04 (m, 3H); 7.08 (s, H); 7.16 (broad d, J=8.2 Hz, H); 7.35 (d, J=8.7 Hz, H); 7.90 (s, H); 7.95-8.00 (m, 5H); 8.30 (d, J=8.7 Hz, 2H). *^{19}F NMR* (400 MHz, $CDCl_3$): δ=-126.15 (m, 2F); -122.73 (m, 2F);-121.80 (m, 6F); -121.23 (m, 2F); -110.84 (t, J=14.3 Hz, 2F); -80.78 (t, J=9.9 Hz, 3F).

I-13: *Elemental analysis* for $C_{67}H_{100}N_4O_{11}Ni$ (1196.22 g/mol); calculated; C 67.27; H 8.43; N 4.68; found C 67.17; H 8.51; N 4.74;
^{1}H NMR (400 MHz, $CDCl_3$): δ=0.84–1.88 (m, 75H); 3.31 (s, 3H); 3.32 (s, 3H); 3.93–4.09 (m, 10H); 6.50 (dd, J=2.2 Hz, J=8.7 Hz, H); 6.74 (d, J=2.2 Hz, H); 6.91 (s, H); 7.02 (s, H); 7.27 (d, J=8.7 Hz, H); 7.38 (s, 2H); 7.76 (s, H); 8.19 (s, H).

II-2: *Elemental analysis* for $C_{69}H_{100}N_2O_9Ni$ (1160.23 g/mol); calculated; C 71.43; H 8.69; N 2.41; found C 71.42; H 8.63; N 2.35;
^{1}H NMR (400 MHz, $CDCl_3$): δ=0.85–1.87 (m, 75H); 3.94-4.06 (m, 10H); 6.39 (d, J=2.2 Hz, H); 6.50 and 7.29 (AB, J=7.0 Hz, 2H); 6.52 (dd, J=2.2 Hz, J=8.9 Hz, H); 6.90 (s, H); 6.97 and 8.12 (AA'BB', J=8.9 Hz, 4H); 7.08 (s, H); 7.09-7.12 (m, 2H); 7.26 (broad s, H); 7.93 (d, J=8.9 Hz, H); 7.97 (s, H).

II-4: *Elemental analysis* for $C_{77}H_{116}N_2O_{10}Ni$ (1288.44 g/mol); calculated; C 71.78; H 9.07; N 2.17; found C 71.84; H 9.02; N 2.21;
^{1}H NMR (400 MHz, $CDCl_3$): δ=0.83–1.85 (m, 90H); 3.92-4.06 (m, 12H); 6.39 and 7.29 (AB, J=6.3 Hz, 2H); 6.61 and 7.57 (AB, J=8.9 Hz, 2H); 6.90 (s, H); 6.95 and 8.11 (AA'BB', J=8.9 Hz, 4H); 7.06-7.09 (m, 3H); 7.25 (s, H); 7.93 (s, H).

II-5: *Elemental analysis* for $C_{69}H_{83}F_{17}N_2O_8Ni$ (1450.07 g/mol); calculated; C 57.15; H 5.77; N 1.93; found C 57.11; H 5.74; N 1.98;
^{1}H NMR (400 MHz, $CDCl_3$): δ=0.84–1.88 (m, 60H); 3.98-4.08 (m, 8H); 6.36 and 7.40 (AB, J=6.7 Hz, 2H); 6.95 (s, H); 6.97 and 8.12 (AA'BB', J=8.9 Hz, 4H); 70.4 (broad s, H); 7.07 (s, H); 7.11-7.13 (m, 2H); 7.21 (broad d, J=8.2 Hz, H); 7.27-7.30 (m, H); 7.95 (s, H); 8.00 (d, J=8.2 Hz, H). *^{19}F NMR* (400 MHz, $CDCl_3$): δ=-126.17 (m, 2F); -122.76 (m, 2F); -121.80 (m, 6F); -121.26 (m, 2F); -110.87 (t, J=14.4 Hz, 2F); -80.80 (t, J=9.9 Hz, 3F).

II-6: *Elemental analysis* for $C_{85}H_{132}N_2O_{11}Ni$ (1416.65 g/mol); calculated; C 72.07; H 9.39; N 1.98; found C 72.04; H 9.48; N 2.02;
^{1}H NMR (400 MHz, $CDCl_3$): δ=0.85–1.88 (m, 105H); 3.95-4.08 (m, 14H); 6.40 (d, J=2.3 Hz, H); 6.50 and 7.29 (AB, J=7.0 Hz, 2H); 6.53 (dd, J=2.3 Hz, J=8.8 Hz, H); 6.90 (s, H); 7.06-7.15 (m, 3H); 7.23 (d, J=2.7 Hz, H); 7.39 (s, 2H); 7.93 (d, J=8.8 Hz, H); 7.97 (s, H).

II-7: *Elemental analysis* for $C_{93}H_{148}N_2O_{12}Ni$ (1544.86 g/mol); calculated; C 72.30; H 9.66; N 1.81; found C 72.24; H 9.73; N 1.85;

^{1}H NMR (400 MHz, $CDCl_3$): δ=0.83–1.86 (m, 120H); 3.93-4.08 (m, 16H); 6.39 and 7.28 (AB, J=6.8 Hz, 2H); 6.66 and 7.56 (AB, J=8.9 Hz, 2H); 6.90 (s, H); 7.06-7.09 (m, 2H); 7.21 (broad s, H); 7.39 (s, 2H); 7.92 (s, H).

II-8: *Elemental analysis* for $C_{85}H_{115}F_{17}N_2O_{10}Ni$ (1706.49 g/mol); calculated; C 59.81; H 6.79; N 1.64; found C 59.76; H 6.87; N 1.61;
^{1}H NMR (400 MHz, $CDCl_3$): δ=0.83–1.86 (m, 90H); 3.94-4.08 (m, 12H); 6.26 and 7.30 (AB, J=6.5 Hz, 2H); 6.92 (s, H); 6.98 (s, H); 7.03-7.04 (m, 2H); 7.12 (broad s, H); 7.17 (broad d, J=8.1 Hz, H); 7.39 (s, 2H); 7.73 (s, H); 8.03 (d, J=8.1 Hz, H). *^{19}F NMR* (400 MHz, $CDCl_3$): δ=-126.22 (m, 2F); -122.80 (m, 2F); -121.80 (m, 6F); -121.30 (m, 2F); -110.91 (t, J=14.4 Hz, 2F); -80.85 (t, J=9.7 Hz, 3F).

II-9: *Elemental analysis* for $C_{66}H_{77}F_{17}N_2O_{10}Ni$ (1439.99 g/mol); calculated; C 55.05; H 5.39; N 1.95; found C 54.98; H 5.44; N 1.93;
^{1}H NMR (400 MHz, $CDCl_3$): δ=0.83–1.86 (m, 45H); 3.40 (s, 3H); 3.57-3.62 (m, 2H); 3.72-3.76 (m, 2H); 3.88-3.97 (m, 6H); 4.03 (t, J=6.6 Hz, 2H); 4.21-4.25 (m, 2H); 6.24 and 7.28 (AB, J=6.6 Hz, 2H); 6.90 (s, H); 6.96-7.06 (m, 15H); 7.12 (d, J=2.2 Hz, H); 7.16 (broad d, J=8.4 Hz, H); 7.70 (s, H); 8.02 (d, J=8.1 Hz, H); 8.11 (d, J=8.9 Hz, 2H). *^{19}F NMR* (400 MHz, $CDCl_3$): δ=-126.15 (m, 2F); -122.76 (m, 2F); -121.80 (m, 6F); -121.26 (m, 2F); -110.87 (t, J=14.3 Hz, 2F); -80.81 (t, J=10.4 Hz, 3F).

II-10: *Elemental analysis* for $C_{69}H_{83}F_{17}N_2O_8Ni$ (1450.07 g/mol); calculated; C 57.15; H 5.77; N 1.93; found C 57.04; H 5.78; N 1.95;
^{1}H NMR (400 MHz, $CDCl_3$): δ=0.84–1.87 (m, 60H); 3.93–3.97 (m, 4H); 3.99 (t, J=6.6 Hz, 2H); 4.04 (t, J=6.6 Hz, 2H); 6.36 and 7.29 (AB, J=6.7 Hz, 2H); 6.85 (s, H); 6.90 and 7.08 (AA'BB', J=9.1 Hz, 4H); 7.04 (broad s, H); 7.05-7.07 (m, 2H); 7.18 (broad d, J=8.3 Hz, H); 7.95-8.01(m, 3H); 8.29 (d, J=2.3 Hz, H). *^{19}F NMR* (400 MHz, $CDCl_3$): δ=-126.12 (m, 2F); -122.72 (m, 2F);-121.76 (m, 6F); -121.20 (m, 2F); -110.86 (t, J=14.0 Hz, 2F); -80.78 (t, J=10.1 Hz, 3F).

II-11: *Elemental analysis* for $C_{75}H_{104}N_4O_9Ni$ (1264.34 g/mol); calculated; C 71.25; H 8.29; N 4.43; found C 71.19; H 8.24; N 4.46;,
^{1}H NMR (400 MHz, $CDCl_3$): δ=0.85–1.86 (m, 75H); 3.92 (t, J=6.6 Hz, 2H); 3.95–4.00 (m, 6H); 4.04 (t, J=6.6 Hz, 2H); 6.39 (d, J=2.2 Hz, H); 6.48 and 7.24 (AB, J=6.7 Hz, 2H); 6.52 (dd, J=2.2 Hz, J=8.9 Hz, H); 6.85 (s, H); 7.06-7.12 (m, 3H); 7.28 (d, J=2.1 Hz, H); 7.91-7.95 (m, 6H); 8.28 (d, J=8.6 Hz, 2H).

II-12: *Elemental analysis* for $C_{75}H_{87}F_{17}N_4O_8Ni$ (1554.18 g/mol); calculated; C 57.96; H 5.64; N 3.61; found C 58.02; H 5.71; N 3.56;
^{1}H NMR (400 MHz, $CDCl_3$): δ=0.84–1.88 (m, 60H); 3.92–4.09 (m, 8H); 6.29 and 7.30 (AB, J=6.6 Hz, 2H); 6.91 (s, H); 6.99-7.04 (m, 4H); 7.06 (s, H); 7.08 (d, J=2.8 Hz, H); 7.19 (broad d, J=8.2 Hz, H); 7.22 (d, J=2.6 Hz, H); 7.77 (s, H); 7.92-7.96 (m, 4H); 8.04 (d, J=8.2 Hz, H); 8.29 (d, J=8.5 Hz, 2H). *^{19}F NMR* (400 MHz, $CDCl_3$): δ=-126.15 (m, 2F); -122.75 (m, 2F);-121.80 (m, 6F); -121.24 (m, 2F); -110.85 (t, J=14.3 Hz, 2F); -80.79 (t, J=9.9 Hz, 3F).

II-13: *Elemental analysis* for $C_{67}H_{100}N_4O_{11}Ni$ (1196.22 g/mol); calculated; C 67.27; H 8.43; N 4.68; found C 67.22; H 8.48; N 4.65;
^{1}H NMR (400 MHz, $CDCl_3$): δ=0.84–1.88 (m, 75H); 3.33 (s, 3H); 3.40 (s, 3H); 3.93–4.08 (m, 10H); 6.91 (s, H); 6.95–6.99(m, 2H); 7.10 (dd, J=2.9 Hz, J=9.2 Hz, H); 7.21 (d, J=2.9 Hz, H); 7.38 (s, 2H); 7.75 (s, H); 8.24 (s, H).

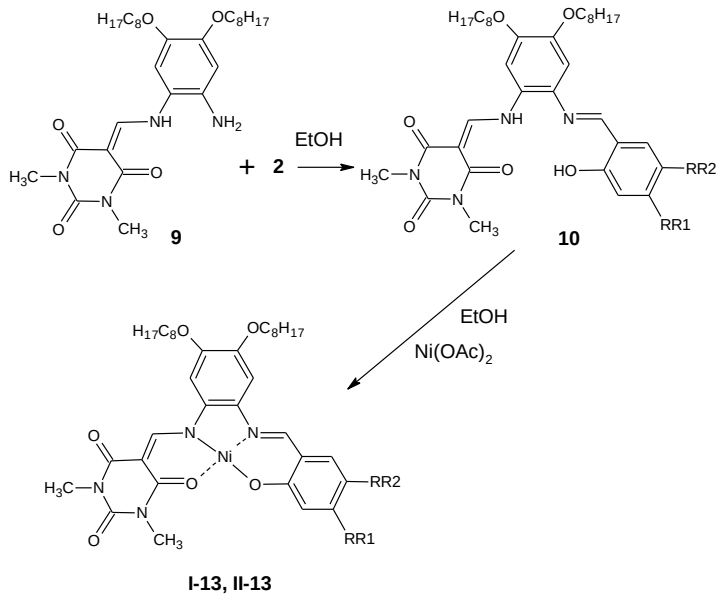

Scheme SI 2. Synthesis of compounds **I-13** and **II-13**.

The way of synthesis of compounds **I-13** and **II-13** is shown in Scheme SI 2. Preparation of the substrate (**9**) applied in this procedure was described in Ref. SI 5.

Complexes I-13 and **II-13:** The synthesis of these complexes was identical as the group of complexes **I-1 – I-12** and **II-1 – II-12**.

Identification of phases and measurements

The mesophases were identified on a basis of characteristic optical textures, using Zeiss Axio Imager A2m polarizing microscope equipped with a Linkam heating stage. The structure of liquid crystalline phases was confirmed by X-ray measurements performed for powder or partially aligned samples with Bruker D8 GADDS diffractometer (CuKα radiation, Geoble mirror monochromator, point collimator, Vantec 2000 area detector), equipped with modified Linkam heating stage. For small angle diffraction experiments Bruker NANOSTAR diffractometer was used (CuKα radiation, cross-coupled Geoble mirrors, 3-pin hole collimation setup, MRI-TCPU heating stage, Vantec 2000 area detector). Phase transition temperatures and enthalpy changes were determined by calorimetric measurements performed with a TA DSC Q200 set up in inert atmosphere. The phase transition temperatures were determined as an onset of peak tangential line. Temperature changes of birefringence was registered with optical set-up based on photoelastic modulator HindsPEM-90 using light of wavelength 633 nm. A cell of thickness 5 μm filled with homogeneously oriented sample was heated in a Linkam heating stage. Complex dielectric permittivity was measured with Wayne-Kerr precision component analyzer 4625.

Supporting experimental results:

Nematic phase

For materials **I-11** and **I-2** in nematic phase X-ray diffraction pattern with diffused signals was registered, the pattern is characteristic for structure with short range positional order. For **I-5** and **I-12** materials in X-ray diffraction pattern coexistence of N phase with crystal phase is observed.

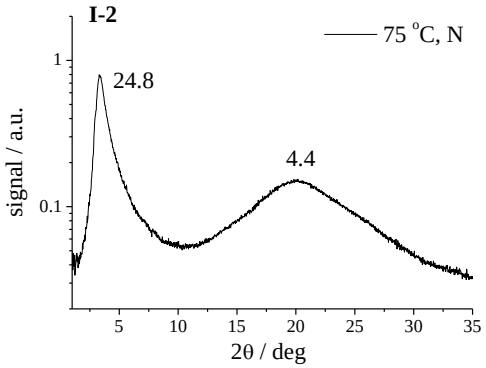

Figure SI 1. XRD signals of N phase in **I-2** compound; periodicity (in Å) corresponding to maxima of the peaks is marked.

In a glass cell covered with rubbed polymer surfactant layers, nearly ideal planar texture, without defects, was observed for nematic phase under polarizing microscope. (Figure SI 2). Upon decreasing temperature, in cells with rubbing direction oriented at 45 degree to the polarizers, the sample color changes consistent with increasing birefringence.

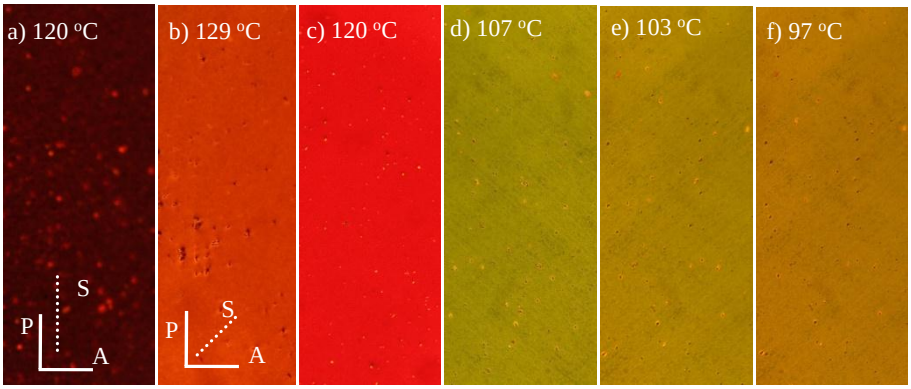

Figure SI 2. Textures of N phase in **I-11** compound, placed in a cell with rubbing direction (S) at a) 0 degree and b) - f) 45 degree to polarizer (P) and analyzer (A) directions, upon changing temperature.

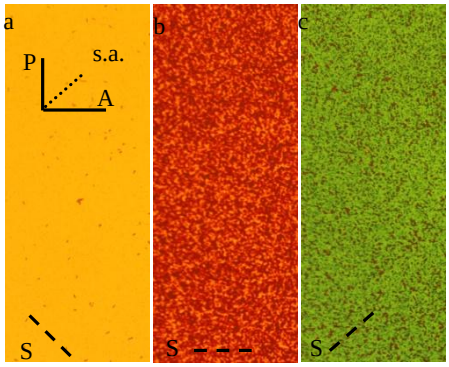

Figure SI 3. Color changes for nematic N phase at 126 °C in **I-11**compound; the 'lambda plate' (λ) was inserted into microscopic optical path with the slow axis (s.a.) at 45 degree to polarizers (P) and analyzers (A); S – is a rubbing direction in the cell.

To verify the molecular arrangement on rubbed support a λ plate was inserted into microscopic optical path with its slow axis oriented at 45° to the direction of polarizer. Upon rotation of the cell, *i.e.* when the cell rubbing direction changes with respect to lambda plate (Figure SI 3), the color of the sample changes *i.e.* if the λ plate is oriented with its slow axis (s.a.) along the rubbing direction (S) the sample becomes green and when slow axis is perpendicular to the rubbing direction the sample

becomes yellow. According to the Michel-Levy chart the green color corresponds to higher birefringence. This points to the positive birefringence of the material *i.e.* the molecules are oriented with their larger molecular dimension (polarizability) along the rubbing directions. In case of rod-like molecules in N phase this means that the average direction of long molecular axis (director) is aligned parallel to the rubbing direction. When it is N_D phase made of disc-like molecules the experiment suggests that discs planes are oriented along rubbing and therefore director (average direction of short molecular axis) is perpendicular to the rubbing. When it were N_{Col} phase we can expect that the columns should be aligned along rubbing and therefore disc-like molecules should be oriented perpendicular to the rubbing. Hence for N_{Col} phase birefringence should be negative that is inconsistent with experimental results.

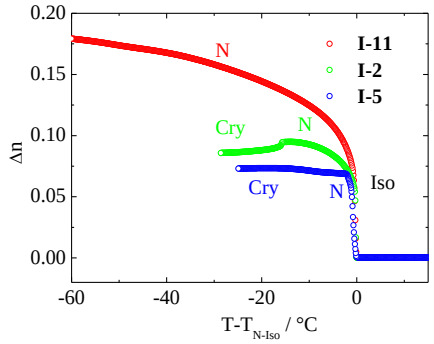

Figure SI 4. Temperature dependence of birefringence for compounds **I-11**, **I-2** and **I-5** in Iso, N, and Cry phases.

The birefringence was calculated form optical retardation measured in the cell of thickness of 5 μm with homogeneously oriented sample at wavelength 633nm (Figure SI 4) For the compounds **I-11,** in which the N phase has broadest temperature range, the birefringence reaches Δn=0.17, for the **I-2** and **I-5** materials, where the nematic phase is nonotropic, the birefringence was considerably lower. The highest difference between ordinary and extraordinary refractive indices for **I-11** compound comes from the highest molecular shape anisotropy.

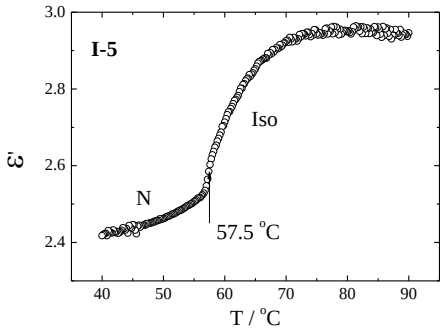

Figure SI 5. Dielectric permittivity ε' of **I-5** material taken at cooling; decrease of ε' at the transition from isotropic to nematic phase indicates that rod-like molecules are oriented parallel to the cell surfaces in the homogenously orientated sample (in N phase).

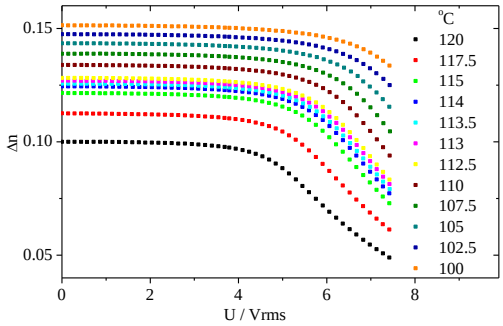

Figure SI 6. Birefringence of **I-11** compound at various temperature under increasing applied voltage.

The birefringence of the material **I-11** in homogeneously oriented sample was also measured under electric field that was applied across cell thickness. The sample exhibits threshold switching behavior and the decrease of birefringence confirms planar to homeotropic reorientation under electric field that is expected for rod-like molecules. For N_D and N_{Col} phases the discotic molecules in homogenous orientation have their long axes perpendicular to the cell surface and no switching of their orientation is expected under electric field.

Columnar phases

The crystallographic data obtained from X-ray studies are collected in Table SI 1.

Table SI 1. Crystallographic distances (in Å) corresponding to X-ray diffraction signals; calculated parameters of hexagonal crystallographic lattice, a (in Å); d_c and d_d – distance between chains and discs, respectively (in Å).

	Phase, temp / °C	Signal / Å	a / Å	d_c / Å	d_d / Å
I-2	N, 75	24.8		4.4	
I-7	Col_{hd1}, 55 Col_{hd2}, 30	24.6 23.7	28.5 27.4	4.4 4.4	3.5 3.4
I-8	Col_{hd}, 200 85	25.8 25.2	29.9 29.2	5.0 4.75	
I-9	Col_{ros}, 85		$a = b =$ 47.0*	5.1	3.4
I-11	N, 100	23.2		4.4	
I-13	Col_{hd}, 200 100	22.9 22.3	26.5 25.7	4.85 4.7	
II-5	Col_{hd}, 160	23.7	26.6	5.0 5	3.3
II-7	Col_{hd}, 100	25.5	29.5	4.4 5	3.5
II-8	Col_{ho}, 100 Col_{ro}, 30	25.2	29.1 a=46.0* b=30.8*	4.9 4.7	3.3 3.3
II-10	Col_{ho}, 120 Col_{ros}, 50	23.00	26.6 $a = b =$ 48.4*		
II-13	Col_{hd}, 150	22.7	26.3	4.6	

*a and b – crystallographic parameters of rectangular lattice

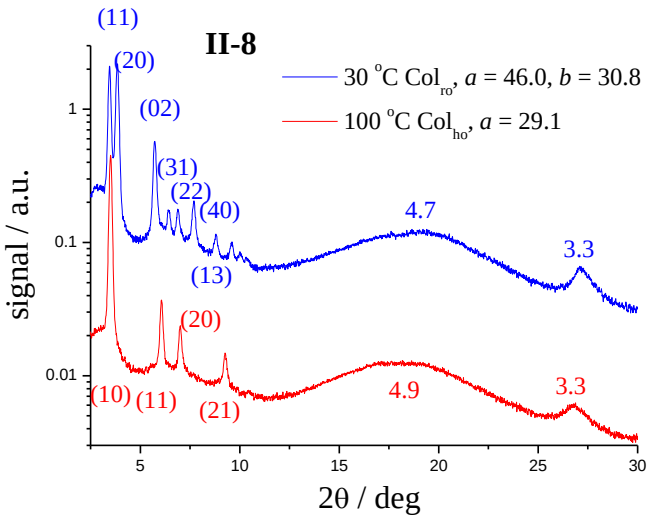

Figure SI 7. XRD patterns of Col$_{ho}$ and Col$_{ro}$ phases in **II-8** compound; at 100 °C *a* – hexagonal lattice parameter and at 30 °C *a* and *b* - rectangular lattice parameters (in Å); also position (in Å) of high angle peaks are marked.

Reentrant isotropic phase

Dielectric measurements show that dielectric constant is similar in Iso and Iso$_{re}$ phases of **II-13** material (Figure SI 8). The decrease observed on cooling in Iso$_{re}$ phase is caused by slow re-crystallization of the sample.

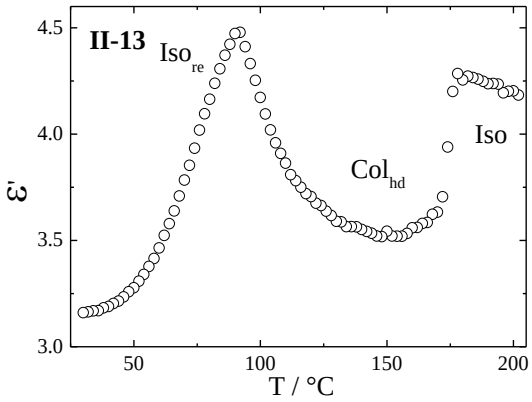

Figure SI 8 Dielectric permittivity for **II-13** material measured on cooling; in Col$_{hd}$ phase molecules are orientated parallel to the cell surfaces.

Superstructure in columnar phase

The X-ray studies show that the transition from Col_{hd} phase to lower temperature Col_{ros} phase is of first order, however accompanied by strong fluctuations that develop already several degree above the transition (Figure SI 9)

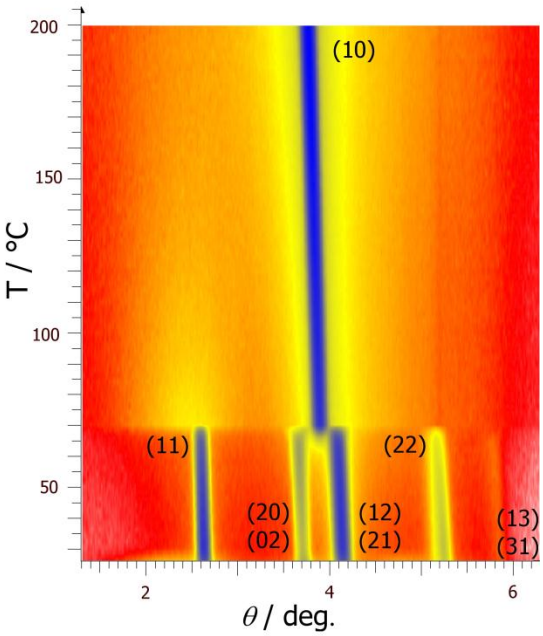

Figure SI 9 temperature evolution of XRD signals for **II-10** material; at higher temperature - Col_{hd} phase, at lower temperature Col_{ros} phase.

The degeneracy of the signal orientation in X-ray pattern can be explained by the different orientation of rectangular initial crystallites of Col_{ros} phase superimposed on the hexagonal structure of Col_{hd} phase (Figure SI 10).

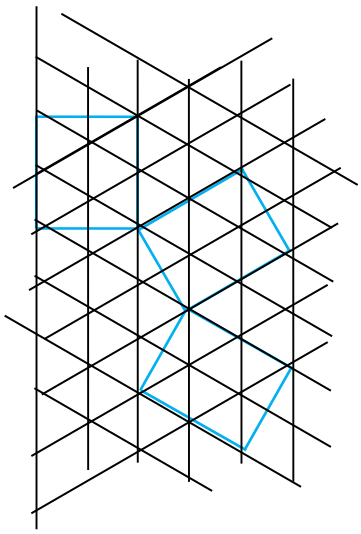

Figure SI 10. Orientation of 'rectangular crystallographic unit cells' of Col_{ros} phase that are superimposed on the hexagonal structure of Col_{hd} phase, leading to the degeneracy of the signal azimuthal positions in X-ray pattern of Col_{ros} phase and apparent 12-fold symmetry of the pattern.

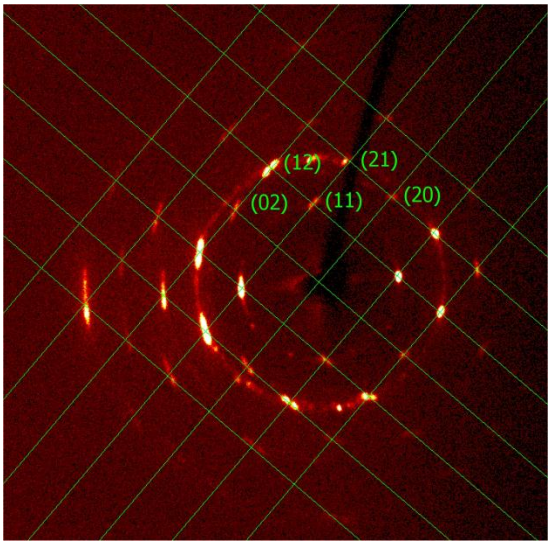

Figure SI 11. 2D XRD pattern of Col_{ros} phase in **I-9** material at 85 °C with sketched reciprocal lattice coming from single domain grown from isotropic liquid.

References

SI 1. A. Krówczyński, J. Szydłowska, D. Pociecha, J. Przedmojski and E. Gorecka, *Liquid Crystals*, 1998, **25**, 117.
SI 2. N. Audic, P. W. Dyer, E. G. Hope, A. M. Stuart and S. Suhard, *Advanced Synthesis and Catalysis*, 2010, **352**, 2241
SI 3. A. Lesac, H. L. Nguen, S. Narančić, U. Baumeister, S. Diele and D. W. Bruce, *Liquid Crystals*, 2006, **33**, 167; B. T. Thaker, and P. Patel, *Molecular Crystals and Liquid Crystals*, 2009, **509**, 173.
SI 4. K. Binnemans, and K. Lodewyckx, *Supramolecular Chemistry*, 2003, **15**, 485.
SI 5. A. Krówczyński, P. Krzyczkowska, M. Salamończyk, E. Gorecka, D. Pociecha and J. Szydłowska, *Liquid Crystals*, 2012, **39**, 729.